Author Manuscript

Author Manuscript

Author Manuscript

Author Manuscript

HHS Public Access

Author manuscript

Nat Immunol. Author manuscript; available in PMC 2017 April 10.

Published in final edited form as:

Nat Immunol. 2016 May ; 17(5): 583–592. doi:10.1038/ni.3389.

T cell-intrinsic ASC critically promotes T_H17-mediated experimental autoimmune encephalomyelitis

Bradley N. Martin[*,1,2], **Chenhui Wang**[*,1,3], **Cun-jin Zhang**[1], **Zizhen Kang**[4], **Muhammet Fatih Gulen**[1], **Jarod A. Zepp**[1], **Junjie Zhao**[1], **Guanglin Bian**[1], **Jeong-su Do**[1], **Booki Min**[1], **Paul G. Pavicic JR**[1], **Caroline El-Sanadi**[5], **Paul L. Fox**[6], **Aoi Akitsu**[7], **Yoichiro Iwakura**[7], **Anasuya Sarkar**[8], **Mark D. Wewers**[8], **William J. Kaiser**[9], **Edward S. Mocarski**[9], **Marc E. Rothenberg**[10], **Amy G. Hise**[11], **George R. Dubyak**[5], **Richard M. Ransohoff**[12,#], and **Xiaoxia Li**[1]

[1]Department of Immunology, Cleveland Clinic Lerner Research Institute, Cleveland, OH, 44195

[2]Department of Pathology, Case Western Reserve University School of Medicine, Cleveland, OH, 44106

[3]Key Laboratory of Molecular Biophysics of the Ministry of Education, College of Life Science and Technology, Huazhong University of Science and Technology, Wuhan 430074, China

[4]Shanghai Institute of Immunology, Shanghai Jiaotong University of School of Medicine, Shanghai, 200025, P.R. China

[5]Department of Physiology and Biophysics, Case Western Reserve University School of Medicine, Cleveland, OH

[6]Department of Cellular and Molecular Medicine, Cleveland Clinic Lerner Research Institute, Cleveland, OH, 44195

[7]Research Institute for Biomedical Sciences, Tokyo University of Science, 2669 Yamazaki, Noda, Chiba 278-0022, Japan

[8]Davis Heart and Lung Research Institute, Ohio State University College of Medicine, Columbus, OH, 43210

[9]Department of Microbiology and Immunology, Emory Vaccine Center, Atlanta, GA, 30322

[10]Division of Allergy and Immunology, Cincinnati Children's Hospital Medical Center. Cincinnati, OH 45229-3039

[11]Pathology and International Health. Case Western Reserve University. Cleveland, OH 44106

Correspondence can be addressed to Dr. Li (lix@ccf.org) or Dr. Ransohoff (rransohoff@gmail.com).

[*]These authors contributed equally to this work.

[#]Current address: Biogen Idec, Cambridge, MA, 02142.

AUTHOR CONTRIBUTIONS STATEMENT

B.N.M. and C.W. did the experiments and analyzed the data; C.J Z., Z. K., M.F.G., J.A.Z., J.Z., C.E.S. and B.L. contributed to the experiments; J.D. and P.P. helped to make the *Cd3e*$^{-/-}$ and *Il1b*$^{-/-}$ bone marrow chimera mice; A.A., Y.L., A.S., M.D.W., W.J.K., E.S.M., M.E.R. and A.G.H. provided reagents and participated in discussion; B.M. and G.R.D contributed reagents, helped to design experiments and helped to edit the manuscript; B.N.M., C.W. and X.L. wrote the manuscript; R.M.R. and X.L. conceived the study, oversaw the experiments and analyzed the data.

COMPETING INTERESTS STATEMENT

The authors declare no competing financial interests.

Author Manuscript Author Manuscript Author Manuscript Author Manuscript

[12]Department of Neurosciences, Cleveland Clinic Lerner Research Institute, Cleveland, OH, 44195

Abstract

IL-1β is critical for T_H17 cell survival, expansion, and effector function *in vivo* during autoimmune responses, including EAE. However, the spatiotemporal role and cellular source of IL-1β during EAE pathogenesis is poorly defined. In the present study, we uncovered a novel T cell-intrinsic inflammasome that drives IL-1β production during T_H17-mediated EAE pathogenesis. TCR activation induced pro-IL-1β expression, while ATP stimulation triggered T cell production of IL-1β via ASC-NLRP3-dependent caspase-8 activation. IL-1R was detected on T_H17 but not T_H1 cells, and ATP-treated T_H17 cells showed enhanced survival compared to ATP-treated T_H1 cells, suggesting autocrine action of T_H17-derived IL-1β. Together, these data reveal a critical role for IL-1β produced by a T_H17 cell-intrinsic ASC-NLRP3-Caspase-8 inflammasome during CNS inflammation.

INTRODUCTION

Multiple sclerosis (MS) is an inflammatory demyelinating disease of the central nervous system (CNS) that affects an estimated 350,000 people in the United States, and some 2.5 million worldwide[1]. Experimental autoimmune encephalomyelitis (EAE) is the most commonly utilized animal model of MS. Studies using the EAE model have helped to define the sequence of immunopathogenic events in the development of autoimmune CNS-directed inflammatory disease[2]. During the initiation stage of EAE, CNS antigen-reactive T cells undergo activation and clonal expansion in the secondary lymphoid organs, while antigen-presenting cells (APCs) simultaneously produce cytokines that regulate the differentiation of effector CD4+ T cells, skewing these cells to classical T_H1 (producing IFN-γ) and T_H17 (producing IL-17, IL-21, GM-CSF and TNF) T cell lineages. Importantly, recent data demonstrate that both T_H1 and T_H17 cells are able to independently induce EAE, possibly through different mechanisms[3–6].

T_H17 cells are generated as a discrete lineage when the peripheral priming microenvironment contains TGFβ and IL-6, and appear to acquire encephalitogenic potential following re-activation and expansion in the presence of IL-1β and IL-23[7–9]. We, along with others, have reported that expression of the IL-1 receptor (IL-1R) is highly induced during T_H17 cell differentiation[10,11]. Mice deficient in IL-1R have been shown to display a significant reduction in EAE disease severity, while mice deficient in IL-1Ra, the endogenous soluble IL-1R antagonist, were shown to have worse disease than wild-type controls[10,12,13]. IL-1β stimulation of T_H17 cells leads to strong and prolonged activation of the mammalian target of rapamycin (mTOR) pathway, which plays a critical role in cell proliferation and survival, and is required for T_H17-dependent EAE pathogenesis[14,15].

The NLRP3 inflammasome consists of NLRP3 linked via a homotypic pyrin domain interaction to the inflammasome adaptor molecule apoptosis-associated speck-like protein containing a C-terminal caspase-activation and recruitment (CARD) domain (ASC). ASC interacts with pro-caspase-1 via a CARD domain, resulting in caspase 1 activation and

Author Manuscript Author Manuscript Author Manuscript Author Manuscript

maturation and production of IL-1β and IL-18. Several independent studies have recently reported a critical role for the NLRP3 inflammasome in EAE pathogenesis[16–18]. However, the spatiotemporal role and cellular source of IL-1β during EAE pathogenesis is poorly defined. Although many previous studies have reported that ASC-dependent inflammasome signaling mediates T cell function during both host defense and autoimmune processes, it has remained unclear whether ASC has any T cell-intrinsic role.

Here, we report that the inflammasome adaptor molecule ASC plays a critical T cell-intrinsic role in the pathogenesis of T_H17-mediated EAE. T cell-intrinsic ASC is required for the effector stage of EAE, and ASC deficiency in T cells impaired T_H17- but not T_H1-mediated EAE. Mechanistically, TCR activation induced pro-IL-1β expression and nuclear-to-cytosolic translocation of ASC; polarized T_H17 cells expressed IL-1R, and produced mature IL-1β in response to ATP via ASC/NLRP3-dependent caspase-8 activation. ATP-treated T_H17 cells showed enhanced survival compared to ATP-treated T_H1 cells, which was abrogated by IL-1Ra, suggesting an autocrine action of T_H17-derived IL-1β. Together, these data suggest a critical role for IL-1β produced by a novel T_H17 cell-intrinsic ASC-NLRP3-Caspase-8 inflammasome during CNS inflammation.

RESULTS

T cell-specific ASC deficiency delayed and greatly attenuated EAE

To investigate whether *Asc* has any T cell-intrinsic role, we bred a mouse strain in which all three exons of the *Pycard* gene (that encodes *Asc*) are flanked by lox(p) sites ($Asc^{f/f}$ mice) onto the *Lck*-cre transgenic mouse strain, which expresses Cre under the control of the *Lck* proximal promoter, generating $Asc^{f/+}Lck$-Cre mice (Fig. 1a and Supplementary. Fig. 1). We generated mice with T cell-specific deletion of *Asc* by further crossbreeding to obtain $Asc^{f/-}Lck$-Cre and littermate control $Asc^{f/+}Lck$-Cre mice (Supplementary. Fig. 2). We tested the impact of T cell-specific *Asc* deletion on neuroinflammation and demyelination by subjecting $Asc^{f/-}Lck$-Cre and littermate control $Asc^{f/+}Lck$-Cre mice to immunization with neuroantigen, $MOG_{35–55}$ peptide. Mice with T cell-specific ASC deficiency had attenuated disease severity compared to controls (Fig. 1b). $Asc^{+/+}$ and $Asc^{+/-}$ mice exhibited similar EAE phenotype upon immunization (data not shown), indicating haploinsufficiency of *Asc* has no impact on EAE phenotype. While $Asc^{f/+}Lck$-Cre developed severe EAE, $Asc^{f/f}Lck$-Cre mice were protected, mirroring the data shown in Fig. 1b (data not shown). Inflammatory mononuclear cell infiltration in the brain, including CD4+ T cells, B cells, neutrophils and macrophages, was similarly reduced in mice with T cell-specific *Asc* ablation (Fig. 1c–d) and the expression of inflammatory cytokine and chemokine expression in the spinal cord was also significantly decreased (Fig. 1e). Histopathological analysis showed reduced infiltrating immune cell accumulation and resultant demyelination in spinal cord of $Asc^{f/-}Lck$-Cre mice compared to controls (Fig. 1f). Together, these data indicate that deletion of *Asc* from T cells greatly protects mice from the pathogenesis of EAE, with a marked attenuation of disease severity.

Author Manuscript Author Manuscript Author Manuscript Author Manuscript

T cell-specific ASC deficiency had no impact on T cell priming

Given the phenotype observed in *Asc*$^{f/-}$*Lck*-Cre mice after immunization with $MOG_{35–55}$ peptide, we hypothesized that ASC in CD4+ T cells might be important for the priming of $MOG_{35–55}$ -reactive T effector populations in the secondary lymphoid organs. However, intracellular staining of T cells obtained from lymph nodes of $MOG_{35–55}$-immunized mice cultured in T_H17- and T_H1-polarizing conditions in the presence of $MOG_{35–55}$ indicated that T cell-specific ASC dificiency had no impact on the frequency and total numbers of IL-17A + and IFN-γ+ CD4+ T cells (Fig. 2a). In addition, supernatants from cultures of $MOG_{35–55}$ -primed lymph node cells from *Asc*$^{f/-}$*Lck*-Cre^{-} mice showed similar levels of IL-17A and IFN-γ as compared to controls (Fig. 2b). Furthermore, *Asc*$^{f/-}$*Lck*-Cre and *Asc*$^{f/+}$*Lck*-Cre sorted naïve CD4+ T cells (CD4+ CD44^{lo}) had a similar capacity to differentiate to T_H1, T_H2, T_H17 and T_{reg} populations in an antigen-independent manner *in vitro* (Fig. 2c–g). Together, these findings suggested that T cell specific ASC deficiency does not impact T cell development, *ex vivo* T cell differentiation, or primary $MOG_{35–55}$ -specific T cell priming *in vivo*.

T cell-intrinsic ASC is required for T_H17-mediated EAE

Given that T cell-specific deficiency attenuated EAE pathogenesis but not T cell priming, we assessed the pathogenic role played by *Asc*-sufficient *and Asc*-deficient T_H1 and T_H17 cells by adoptive transfer into naïve recipients. We found that wild-type recipients receiving *Asc*$^{f/-}$*Lck*-Cre cells re-stimulated under T_H1-promoting conditions developed similar disease as those receiving T_H1 cells from *Asc*$^{f/+}$*Lck*-Cre mice (Fig. 3a). Analysis of the infiltrating mononuclear cell population in the brains of these mice showed no difference in the accumulation of CD4+ or CD8+ T cells, macrophages, neutrophils, or B-cells, consistent with the clinical scores (Fig. 3b). Wild-type mice receiving *Asc*$^{f/-}$*Lck*-Cre cells re-stimulated under T_H17-promoting conditions developed disease with reduced severity than those receiving T_H17 cells from *Asc*$^{f/+}$*Lck*-Cre mice (Fig. 3c). Surface staining of the brain mononuclear cell population revealed that the numbers of CD4+ T cells, macrophages, and neutrophils were also reduced in mice receiving *Asc*-deficient T_H17 cells (Fig. 3d). Histopathological analysis also reflected this reduced inflammatory cell infiltration, along with a reduction in demyelination in recipient mice receiving ASC-deficient T_H17 cells (Fig. 3e). Taken together, these results suggest that T cell-intrinsic ASC is required for T_H17- but not T_H1-mediated EAE. We then sorted CD4+ T_H17 cells by flow cytometry from MOG-immunized *Asc*$^{f/-}$*Lck*-Cre and *Asc*$^{f/+}$*Lck*-Cre control mice and adoptively transferred into irradiated wild-type recipients. The peripheral priming of MOG-reactive T_H17 cells was equivalent in *Asc*$^{f/-}$*Lck*-Cre and *Asc*$^{f/+}$*Lck*-Cre control mice (Fig. 2a, b and Supplementary. Fig. 3a). Recipients (CD45.1 mice) of sorted *Asc*$^{f/-}$*Lck*-Cre CD45.2-CD4+ T_H17 cells showed much reduced EAE phenotype as compared to recipients of *Asc*$^{f/+}$*Lck*-Cre CD45.2-CD4+ T_H17 cells (Supplementary. Fig. 3), together suggesting that *Asc* in CD4+ T_H17 cells is required for the effector stage of EAE development.

Intracellular staining of brain-infiltrating mononuclear cells revealed that the percentage and absolute number of both IL-17- and IFNγ- secreting cells were decreased in mice receiving T_H17 cells from *Asc*$^{f/-}$*Lck*-Cre mice compared to those from *Asc*$^{f/+}$*Lck*-Cre mice (Fig. 3f). Previous studies reported that during the development of EAE, IFN-γ and other pro-

Author Manuscript Author Manuscript Author Manuscript Author Manuscript

inflammatory cytokines (GM-CSF and TNF) in the spinal cord were produced almost exclusively by cells that had produced IL-17 (ex- T_H17 cells)[19], suggesting that the reduction in IFN-γ-secreting cells in the CNS of mice receiving *Asc*$^{f/-}$*Lck*-Cre T_H17 cells might be due to reduced T_H17 and/or ex- T_H17 cells in the CNS. In support of this, *Asc*$^{f/-}$*Lck*-Cre CD4+ T cells sorted from the brains of recipient mice were indeed defective in their secretion of key pro-inflammatory cytokines, including those reported to be produced by T_H17 and ex-T_H17 cells (*Il17a*, *Ifng*, *Csf2* and *Tnf*) and, most interestingly, IL-1β (Fig. 3g). Taken together, these findings indicated that ASC-deficient T_H17 cells are markedly deficient in their production of key pro-inflammatory cytokines in the CNS.

To exclude the possibility that T cell-intrinsic ASC deficiency impacts CD4+ T_H17 migration to the CNS, we adoptively transferred MOG-primed T_H17 cells from *Asc*$^{f/-}$*Lck*-Cre and *Asc*$^{f/+}$*Lck*-Cre mice into *Rag1*$^{-/-}$ recipient mice. We found that T_H17 cells from mice with T cell-specific ASC deficiency egressed from the spleen and migrated to the CNS normally during the first wave of CNS infiltration (days 3 and 6 post-transfer) (Fig 3h–i). However, by day 10 after adoptive transfer, CD4+ T cell numbers in the CNS were reduced in mice receiving T_H17 cells from *Asc*$^{f/-}$*Lck*-Cre mice, suggesting that T_H17 cell survival/expansion in the CNS might be defective in the absence of ASC. In support of this, Ki67 staining in the spinal cord revealed proliferating infiltrated CD4+ T cells after adoptive transfer of wild-type T_H17 cells, which was markedly reduced in mice receiving ASC-deficient- T_H17 cells (Fig. 3j).

T_H17 cells actively secrete mature IL-1β

Given that ASC-deficient T_H17 cells failed to expand and secrete pro-inflammatory cytokines – including IL-1β - in the CNS, we explored whether ASC might serve as an adaptor for inflammasome activation in T_H17 cells. During *in vitro* T_H17 cell differentiation, pro-IL-1β expression was strongly induced (Fig. 4a–b). ATP is released by cells during stress and cell death, and is abundant in the extracellular space in the CNS, where it also acts as a key excitatory neurotransmitter[20–22]. We thus speculated that the observed pro-IL-1β in T_H17 cells might undergo processing in response to stimulation with extracellular ATP. Indeed, *in vitro* polarized T_H17 cells were capable of processing and secreting the active form of IL-1β upon ATP stimulation (Fig. 4c–g), although the amount of mature IL-1β produced by T_H17 cells was less compared to that produced by macrophages (Supplementary. Fig. 4). However, in ASC- and NLRP3-deficient T_H17 cells, IL-1β processing was completely abolished (Fig. 4c–d, g). Caspase-1 is the prototypical interleukin-1β converting enzyme in myeloid-lineage cells, and the regulation and function of the canonical caspase-1 inflammasome has been the subject of intense research. However, T_H17 cells deficient in both caspase-1 (*Casp1*$^{-/-}$) and caspase-11 (*Casp4*$^{-/-}$; called '*Casp11*$^{-/-}$' here) showed only a moderate reduction in IL-1β production as compared to controls (Fig. 4e,g). Caspase-8 was recently identified as a non-canonical inflammatory caspase in myeloid-lineage cells, and has been shown to be capable of processing pro-IL-1β[23–25]. This caspase-8-dependent activity was also shown to be important for T_H17 cell-mediated host defense[24]. Additionally, caspase-8 has been revealed to play a critical non-apoptotic role in T cells[26–31]. We thus speculated that in T_H17 cells, caspase-8 might participate in an ASC-dependent non-canonical inflammasome capable of processing pro-

Author Manuscript Author Manuscript Author Manuscript Author Manuscript

IL-1β. In response to ATP stimulation, IL-1β production was significantly reduced in T_H17 cells from *Caspase-8*$^{-/-}$*Ripk3*$^{-/-}$ mice compared to those from *Caspase-8*$^{+/-}$*Ripk3*$^{-/-}$ mice, implying a role for caspase-8 in T_H17 cells for the ASC-dependent processing of pro-IL-1β (Fig. 4f,g). In support of this, peptide inhibitor of caspase-8 but not caspase-1 specifically blocked IL-1β production in T_H17 cells (Fig. 4h). Analysis of caspase-8 activation demonstrated that extracellular ATP indeed activates caspase-8 in a dose-dependent manner, which was substantially reduced in ASC- and NLRP3-deficient T_H17 cells (Fig. 4i). Given the finding that ATP stimulation of T_H17 cells induced processing of pro-IL-1β in an ASC- and caspase-8-dependent manner, we sought to further define the responsible molecular complex. Stimulation of T_H17 cells with ATP induced the recruitment of both caspase-8 and NLRP3 - but not caspase-1 - to ASC, suggesting that an ASC-NLRP3-caspase-8 complex forms in response to ATP stimulation in T_H17 cells (Fig. 4j).

T_H17-derived IL-1β supports cell survival via an autocrine manner

We next sought to examine the mechanism by which T_H17-polarizing conditions induce pro-IL-1β expression in T cells. Since all T helper cell populations also require TCR stimulation for their initial activation and differentiation from the naïve state, we first tested whether IL-1β expression was shared by these other T cell lineages. Interestingly, we found that Th0, T_H1, and T_H17 cells all showed up-regulation of *Il1b* and *Nalp3* mRNA expression (Fig. 5a–b), a process that has been shown in myeloid cells to be strictly regulated, and which is required for optimal inflammasome activation[32]. Additionally, *Il18* mRNA levels were undetectable in T_H0 and T_H17 cells, with very low expression in T_H1 cells (Fig. 5a). ASC deficiency had no impact on expression of *Il1b, Il18* and *Nalp3* mRNA in T_H0, T_H1 and T_H17 cells (Fig. 5a). ASC, which was located primarily in the nucleus of resting naïve CD4+ T cells, translocated to the perinuclear area in response to TCR stimulation, reflecting what we and others have observed in murine macrophages (Fig. 5c)[33,34]. Further stimulation of these cells with ATP resulted in the formation of large perinuclear ASC specks, which are a well-described marker of inflammasome formation (Fig. 5c). We further found that all three tested T helper lineages robustly activated caspase-8 and produced mature IL-1β following ATP treatment, which was abolished in the corresponding NLRP3- and ASC-deficient T cells (Fig. 5d,e).

Given these data indicating that inflammasome-mediated IL-1β production is not restricted to a particular CD4+ T cell lineage, which was in contrast to our observation that T cell-intrinsic ASC is specifically required for T_H17-mediated neuroinflammation, we sought to examine the functional T_H17 cell-specific role of the ASC-dependent inflammasome. We and others previously reported that IL-1R signaling mediates T_H17 cell maintenance through promotion of cell survival and proliferation[14,15,35]. *Il1r1* gene expression was specifically induced during *in vitro* T_H17- but not T_H1- cell differentiation (Fig. 5f–g; i–j). Upon MOG immunization, IL-1R expression was detected in IL-17$^+$ CD4$^+$ T cells, but not in IFN-γ$^+$ CD4$^+$ T cells (Fig. 5h; 5k). We therefore hypothesized that IL-1β produced by T_H17 cells might act on IL-1R$^+$ T_H17 cells in an autocrine fashion. To test this hypothesis, we examined T_H1 and T_H17 cell survival following 8 hours of ATP stimulation. While both T_H1 and T_H17 cells exhibited caspase-8 activation and IL-1β production, ATP-treated T_H17 cells showed significantly increased cell survival compared to ATP-treated T_H1 cells, which was

Author Manuscript Author Manuscript Author Manuscript Author Manuscript

abrogated by deficiency of ASC, NLRP3, or IL-1β, or by addition of IL-1 receptor antagonist (IL-1Ra) (Fig. 5l). These results suggest that T_H17-derived IL-1β may act in an autocrine fashion to promote survival and proliferation of T_H17 cells with high IL-1R expression (Supplementary. Fig. 5).

CD4+ T cell-derived IL-1β is critical for EAE pathogenesis

To further examine the impact of T_H17 cell-derived IL-1β during EAE, we transferred wild-type or *Il1b*$^{-/-}$*Il18*$^{-/-}$ CD4+ T cells into *Rag1*$^{-/-}$ mice, followed by $MOG_{35–55}$ immunization of the recipients. We found that mice reconstituted with *Il1b*$^{-/-}$*Il18*$^{-/-}$ CD4+ T cells were significantly protected from EAE development compared to controls (Fig. 6a). The mRNA expression of *Il17A* and *Ifng*, as well as their target genes, was significantly decreased in the spinal cords of *Il1b*$^{-/-}$*Il18*$^{-/-}$ CD4+ T cell recipients (Fig. 6b). Inflammatory mononuclear cell infiltration in the CNS, including CD4+ T cells, was also dramatically reduced in *Il1b*$^{-/-}$*Il18*$^{-/-}$ CD4+ T cell recipient mice (Fig. 6C). Histopathological analysis of lumbar spinal cords from *Il1b*$^{-/-}$*Il18*$^{-/-}$ CD4+ T cell recipients showed reduced infiltrating immune cell accumulation and marked protection from demyelinating lesion development (Fig. 6d). Since pro-IL-18 was only slightly induced in T_H1 and not detected in T_H17 cells (Fig. 5a), these results suggested that CD4+ T cell-derived IL-1β is probably critical for EAE pathogenesis. We indeed found that mice reconstituted with *Il1b*$^{-/-}$ CD4+ T cells were almost completely protected from EAE development (Fig. 6e–g), mirroring the results in *Il1b*$^{-/-}$*Il18*$^{-/-}$ CD4+ T cell recipients. Taken together, these results confirm that CD4+ T cell-derived IL-1β is critical for EAE pathogenesis. As an alternative approach to *Rag1*$^{-/-}$ recipient mice, we generated mixed chimeras using *Cd3e*$^{-/-}$ bone marrow together with either wild-type or *Il1b*$^{-/-}$ bone marrow to assess the function of T cell-derived IL-1β. Lethal irradiated WT mice were reconstituted with WT+*Cd3e*$^{-/-}$ bone marrow or *Il1b*$^{-/-}$+*Cd3e*$^{-/-}$ bone marrow. Six weeks after reconstitution, mice were immunized with $MOG_{35–55}$ peptide. The recipient mice received WT+*Cd3e*$^{-/-}$ BM developed EAE, whereas the recipient mice received *Il1b*$^{-/-}$+*Cd3e*$^{-/-}$ BM were protected from EAE (Supplementary. Fig. 6). These results independently validated the critical role of T cell-derived IL-1β in EAE pathogenesis.

Given the potential role of IL-1β in promoting chemokine signals[17], we completed a timecourse analysis to examine the trafficking of donor *Il1b*$^{-/-}$*Il18*$^{-/-}$ CD4+ T cells to the CNS following MOG immunization. The results indicated that T cell-intrinsic IL-1β is dispensible for the first wave of T cell infiltration to the brain and spinal cord, as we observed no defect in CD4+ T cell egression from the spleen or migration to the CNS over the first 3–6 days post-immunization (Fig. 7a). However, by day 10 after adoptive transfer, CD4+ T cell numbers in the CNS were dramatically reduced in mice receiving CD4+ T cells from *Il1b*$^{-/-}$*Il18*$^{-/-}$ mice (Fig. 7a), suggesting CD4+ T cell-derived IL-1β might play an important role in the survival/proliferation of CD4+ T cells in the CNS during EAE. In support of this, Ki-67 immunofluorescent staining of spinal cord tissue revealed a significant reduction of proliferating CD4+ T cells in the absence of T cell-derived IL-1β (Fig. 7b). Flow cytometry indicated that 79% of CD4+ T cells with high IL-1R in the CNS of mice receiving wild-type CD4+ T cells were Ki67+ proliferating cells ($IL\text{-}1R^{hi}Ki67^{+}CD4^{+}$ T cells), whereas only 28% of CD4+ T cells with low IL-1R were Ki67+ cells. These

Author Manuscript Author Manuscript Author Manuscript Author Manuscript

IL-1R^{hi}Ki67^{+}CD4^{+} T cells were diminished in mice receiving CD4+ cells from *Il1b*$^{-/-}$*Il18*$^{-/-}$ mice (Fig. 7c). While previous studies reported that T cell-intrinsic IL-1R signaling is required for T_H17 cell survival/proliferation, the study here indicated that T cell-derived IL-1β is necessary to maintain the proliferation of CD4+ T cells in the CNS. In addition, between days 3, 6, and 10 of EAE development, mice that received wild-type CD4+ T cells showed a marked induction in IFN-γ and GM-CSF gene expression in the spinal cord, while IL-17A and IL-1R gene expression increased proportionally (Fig. 7d). This progressive cytokine induction in the CNS during the course of EAE was abolished in mice receiving CD4+ cells from *Il1b*$^{-/-}$*Il18*$^{-/-}$ mice, indicating the critical role of T cell-derived IL-1β in driving production of pro-inflammatory cytokines to promote CNS inflammation (Fig. 7d). The effect of IL-1- and IL-18-deficiency on T cell percentages in the CNS seems much less marked than for ASC-deficiency, suggesting that ASC might also be involved in non-inflammasome functions.

DISCUSSION

We used T cell-specific genetic deletion of the inflammasome adaptor molecule ASC and found that ablation of ASC in T cells conferred robust protection from EAE development following immunization of mice with $MOG_{35–55}$, while having no impact on the activation and expansion of $MOG_{35–55}$-reactive T_H1 and T_H17 cells in the secondary lymphoid organs. Adoptive transfer of T_H1- and T_H17-polarized $MOG_{35–55}$-reactive cells showed that the protective effect of T cell ASC deficiency was specific to T_H17-, but not T_H1-mediated neuroinflammation. This study demonstrates the critical role of T cell-intrinsic inflammasome in T_H17-mediated EAE pathogenesis.

T_H17-polarized ASC-deficient T cells isolated from the brains of recipient mice were markedly defective in their ability to secrete key pro-inflammatory cytokines, including IL-17A, IFN-γ, GM-CSF, TNF, and IL-1β. Intriguingly, a recent report demonstrated that human CD4+ T cells also process IL-1β in an ASC/NLRP3-dependent manner in response to HIV infection[36]. In addition, findings from the murine EAE model have suggested that IL-1β stimulation actually induces the secretion of IL-17A, IFN-γ, GM-CSF, and TNF from T_H17-polarized brain-infiltrating cells[19]. We further found that T_H17 cells differentiated in vitro highly express both IL-1R and pro-IL-1β, and that this pro-IL-1β can be processed and secreted in response to stimulation with extracellular ATP in a manner dependent on both ASC and NLRP3. Seeking to identify the caspase responsible for ATP-mediated IL-1β production by T_H17 cells *in vitro*, we found that while caspase-1/11 deficiency had minimal effect on IL-1β processing, IL-1β maturation and secretion was abrogated by genetic deletion of caspase-8. This data is surprising, since caspase-1 is expressed in T cells. The fact that pro-caspase-1 was not recruited to ASC upon ATP stimulation suggests the possibility that caspase-1 might be suppressed or sequestered from ASC by an unknown mechanism in murine CD4+ T cells. Future studies are required to elucidate the molecular mechanism for the selective recruitment of caspase-8 to ASC in this context.

An abundance of previously published reports support the notion that IL-1β is critical for the expansion and survival of MOG-reactive T cells in the secondary lymphoid organs[12,14–16,37,38]. However, following immunization of *Asc*$^{f/-}$*Lck*^{Cre} mice with MOG, we

Author Manuscript Author Manuscript Author Manuscript Author Manuscript

did not observe any defect in antigen-dependent T_H17 or T_H1 cell polarization in the spleen, suggesting that IL-1β production by T cells is dispensable for MOG-induced priming in the periphery. It is therefore likely that IL-1β produced by macrophages and dendritic cells in the peripheral environment is sufficient to support initial T_H17 cell priming and expansion. However, we found that while ASC-deficient T_H17 cells are normal in their priming, egress from the spleen, and first-wave infiltration of the CNS following adoptive transfer, they fail to expand and to induce recruitment of second-wave effector cell populations in the CNS. Furthermore, *Il1b*$^{-/-}$ *Il18*$^{-/-}$ CD4+ T cells also show marked defects in proliferation and effector function in the CNS and *Rag*$^{-/-}$ mice reconstituted with *Il1b*$^{-/-}$ CD4+ T cells were protected from EAE development. Taken together, given the specific IL-1R expression in T_H17 cells, these results suggest that ASC-dependent production of IL-1β by T cells in the CNS might be necessary for effective T_H17 cell proliferation and effector cell recruitment.

Of particular note is the finding that both IL-17A- and IFN-γ-producing CD4+ T cell populations were reduced in the absence of T cell-intrinsic ASC. This finding mirrors a recent report that elegantly demonstrated the plasticity of T_H17 cells during EAE pathogenesis[19]. In that study, the authors used an IL-17 promoter-driven T_H17 lineage-tracing reporter system to show that following MOG immunization, classical T_H1 IFN-γ-producing cells were present at a ~1:1 ratio with T_H17-lineage IL-17A-producing cells in the draining lymph nodes. However, after arrival in the CNS, classical T_H1 lineage cells rapidly disappeared by day 15 post-immunization. On the other hand, some T_H17 cells were converted to IL-17- IFN-γ+ cells, so called ex- T_H17 cells, which actually became the dominant IFN-γ-producing cell population in the spinal cord. The IFN-γ-secreting ex- T_H17 cells continue to express IL-1R, while classical T_H1 cells do not. As we observed dramatic defects in both IFN-γ and IL-17A production (and the other inflammatory cytokines) by ASC- and IL-1-deficient CD4+ T cells in the brain, implicating the critical role of T cell-derived IL-1β and consequent IL-1 signaling in T_H17 and ex- T_H17 cells during EAE. T_H1 cells, which lack IL-1R expression, fail to receive the important survival signal provided by T cell-derived IL-1β in the CNS, possibly putting them at a relative disadvantage to T_H17 and ex- T_H17 cells.

In summary, this study is the first to report that T cell intrinsic inflammasome activity drives IL-1β production via caspase-8 activation, and is required for the pathogenic role of T_H17-mediated CNS inflammation. Our findings lead us to speculate that chronic inflammation and tissue destruction in the CNS during EAE provides a prolonged danger signal, potentially in the form of extracellular ATP, to activate ASC-NLRP3-Caspase-8-dependent IL-1β production in T cells. T cell-derived IL-1β in turn promotes the survival/expansion of IL-1R+ $T_H17$cells; and IL-1β stimulation of T_H17 cells also promotes secretion of key pro-inflammatory cytokines, resulting in amplification of the T_H17-mediated inflammatory cascade. This novel model of IL-1β- T_H17 axis yields possible new therapeutic strategies for inhibition of CNS inflammation.

Author Manuscript Author Manuscript Author Manuscript Author Manuscript

METHODS

Mice

B6(Cg)-Tg(Lck-Cd1d1)1Aben/J mice[41] (C57BL/6 background) were purchased from Jackson Laboratory (stock number 019418). *Asc*$^{flox/flox}$ mice were generated by targeting the entire open reading frame of the *Pycard* gene on chromosome 7 for conditional deletion. Targeting vector was generated with a pCR4.0 backbone, and C57BL/6 embryonic stem cells were microinjected and screened by Southern hybridization for presence of the mutant allele. Both the targeting vector and the conditional knockout mice were designed and generated by Caliper Discovery Alliances & Services, which is now part of Taconic. *Asc*$^{-/-}$, *Nlrp3*$^{-/-}$ and *Il1b*$^{-/-}$ mice were described previously[42,43]. *Il1b*$^{-/-}$*Il18*$^{-/-}$ mice were described previously[44]. CD45.1 congenic mice were bought from Jackson Laboratory (002014). *Rag1*$^{-/-}$ mice were bought from Jackson Laboratory (002216). *Casp1*$^{-/-}$*Casp11*$^{-/-}$ mice were bought from Jackson Laboratory (016621)[45]. *Cd3e*$^{-/-}$ mice were bought from Jackson Laboratory (004177). Thy1.1^{+} mice bought from Jackson Laboratory (000406). *Casp8*$^{-/-}$ *Ripk3*$^{-/-}$ and control mice were described previously[46]. All of the mice used in this study were female. For all experiments, mice were 10–12 weeks of age, with age-matched littermates used as experimental groups, and 5 mice pre group. Mice were housed under specific pathogen–free conditions. Experimental protocols were approved by the Institutional Animal Care and Use Committee of the Cleveland Clinic.

Reagents

Anti-ASC (1:1000, N-15-R) was purchased from Santa Cruz Biotechnology. Anti-ASC (1:1000, 2EI-7) was purchased from Milipore. Anti-IL-1β (1:1000, 3ZD) was got from Biological Resources Branch of the NIH. Anti-IL-1β (1:1000, AF-401-NA) was purchased from R&D. Anti-Caspase8 (1:1000 for all three antibodies, 4927, 1G12 and PA1-29159) were purchased from Cell Signaling Technology, Adipogen and ThermoFisher Scientific. Anti-NLRP3 (1:500, H-66) was purchased from SANT CRUZ Biotechnology. Anti-Actin (1:5000, A-2228) was purchased from Sigma. Anti-Ki67 (1:1000, ab15580) was purchased from Abcam. Anti-CD45-APC (1:500, 103112), Anti-CD45.2-PE/cy7 (1:500,104) and Anti-F4/80-FITC (1:200, 123108) were purchased from Biolegend. Anti-CD4-FITC (1:200, L3T4), Anti-Ly6C-PE (1:300, HK1.4), Anti-IFN-γ-FITC (1:200, XMG1.2), Anti-CD3 (1:1000, 145-2C11), Anti-CD28 (1:1000, 37.51), Anti-IL-4-FITC (1:200, BVD6-24G2) and Anti-FOXP3-PE (1:300, FJK-16S) were purchased from eBioscience. Anti-IL-17A-PE (1:300, 559502), Anti-CD8-PE (1:300, 553041) and Anti-Ly6G-PE (1:300, 1A8) were purchased from BD. Anti-IL-1R/CD121a (1:500, clone JAMA-147, catalog #113505) was purchased from Biolegend. Luxol Fast Blue MBS Solution (26681) was purchased from Electron Microscopy Sciences. Caspase-8 Flica (Kit#99) was purchased from ImmunoChemistry. YVAD-fmk (ALX-260-154-R100) and IETD-fmk (550380) were purchased from Enzo and BD. Anti-IL-1β-PE antibody (1:300, IC4013P) was purchased from R&D. IL-1Ra (anakinra) was purchased from AMGEN.

Induction and assessment of EAE

Active EAE was induced and assessed as previously described[39]. Adoptive transfer (passive) EAE was also induced as previously described[40]. Briefly, recipient mice were injected with

Author Manuscript Author Manuscript Author Manuscript Author Manuscript

3.0×10^7 polarized MOG_{35-55}-specific T_H1 or T_H17 cells 4 hours after 500 Rads sublethal irradiation. To prepare MOG_{35-55}-specific polarized T cells, donor mice were immunized with MOG_{35-55} subcutaneously; draining lymph node cells were prepared from donor mice 10 days after immunization. Cells were cultured for 5 days with MOG_{35-55} at a concentration of 25 μg/ml under either T_H1-polarizing conditions (20 ng/ml IL-12, R&D; 2 μg/ml anti-IL-23p19, eBioscience) or T_H17-polarizing conditions (20 ng/ml IL-23, R&D). The clinical score was assessed in double-blinded manner. For the sample size, we performed power analysis for the clinical score of EAE, which has an average of 25% coefficient of variance. We determined that with n=15 mice we had 90% power to detect 30% difference between the groups.

In vitro CD4+ T cell differentiation

For T_H17 cell differentiation, naive $CD4^+CD44^{lo}$ T cells from C57BL/6, *Asc*$^{f/-}$*Lck*-Cre, *Nlrp3*$^{-/-}$, *Casp1*$^{-/-}$/*Casp11*$^{-/-}$, *Casp8*$^{+/-}$*Ripk3*$^{-/-}$ and *Casp8*$^{-/-}$*Ripk3*$^{-/-}$ mice were sorted by flow cytometry and activated with plate-bound 1 mg/ml anti-CD3 and 1 mg/ml anti-CD28 and in the presence of 2 ng/ml TGF-β (Peprotech), 20 ng/ml IL-6 (Peprotech), 5 μg/ml anti-IL-4 (11B11), and 5 μg/ml anti-IFN-γ (XMG 1.2). For T_H1 cell differentiation, FACS-sorted naïve ($CD4^+CD44^{lo}$) CD4+ T cells were cultured on an anti-CD3/CD28 coated plate in the presence of 20 ng/ml IL-12 (Peprotech) and 5 μg/ml anti-IL-4 for 3 days. For T_H2 cell differentiation, FACS-sorted naïve ($CD4^+CD44^{lo}$) CD4+ T cells were cultured on an anti-CD3/CD28 coated plate in T_H2-polarizing (IL-4 (10 ng/ml) and anti-IFN-γ (10 μg/ml)) condition for 3 days. For Treg cell differentiation, FACS-sorted naïve ($CD4^+CD44^{lo}$) CD4+ T cells were cultured on an anti-CD3/CD28 coated plate in the presence of TGFβ (5ng/ml) for 3 days.

Inflammasome activation in CD4+ T cells

FACS-sorted naive $CD4^+CD44^{lo}$ T cells were polarized to the indicated T helper lineage *in vitro* for 3 days. For simulation with ATP, cells were washed and re-suspended in 200 μl low-serum 1640 RPMI media (0.1% of serum) containing the indicated concentration of ATP. For detection of inflammasome activation by immunoblot analysis, we followed the protocol described previously[47]. Briefly, cells were lysed by adding 10× Cell Lysis Buffer (10% Nonidet P-40, 20mM DTT and 10× protease inhibitors) to the well that contains both the cells and culture media (i.e. without removing the condition medium) to a final concentration of 1% Nonidet P-40, 2mM DTT and protease inhibitors. Cells were then lysed (in the presence of culture medium) on ice for 30 minutes, and spun at 16,000 rpm. Protein concentration of the total lysate was measured. 4× Laemlli buffer was then added to the lysate, samples were boiled and approximately 20 μg of sample was run on 12% SDS-PAGE gel, followed by immunoblot analysis.

Reconstitution of T cells in *Rag1*$^{-/-}$ mice and active induction of EAE

2×10^6 FACS-sorted $CD4^+$ T cells from wild-type, *Il1b*$^{-/-}$/*Il18*$^{-/-}$ mice or *Il1b*$^{-/-}$ were i.v. transferred into *Rag1*$^{-/-}$ mice. On days 1 and 4 after CD4+ T cell reconstitution, mice were immunized subcutaneously in the abdominal flank with 200 mg MOG_{35-55} and 400 mg Mycobacteria tuberculosis H37RA (Difco) in 400 μl of an emulsion of equal volumes of

Author Manuscript Author Manuscript Author Manuscript Author Manuscript

water and complete Freund's adjuvant (Difco). Each mouse also received 0.4 mg of purified Bordetella pertussis toxin in 200 μl PBS i.p. on days 0 and 4.

Generation of chimera mice

To generate *Cd3e*$^{-/-}$*Il1b*$^{-/-}$ and *Cd3e*$^{-/-}$*Il1b*$^{+/-}$ chimera mice, 15×10^6 bone marrow cells from *Cd3e*$^{-/-}$ and *Il1b*$^{-/-}$ or *Il1b*$^{+/-}$ bone marrow were injected into irradiated wild-type mice (550 Rads×2 times) by i.v. injection (15×10^6 cells per recipient mouse). Recipient mice were allowed to recover for 6 weeks, followed by active immunization as previously described[39].

Histological analysis

All spinal cord tissue sections used here were 5 μm thick. For paraffin-embedded tissue, spinal cords collected from phosphate-buffered saline–perfused mice were fixed in 10% formalin and then dehydrated with 70% alcohol. Sections were stained with either hematoxylin and eosin or Luxol fast blue to evaluate inflammation and demyelination, respectively.

Real-time PCR

Total RNA was extracted from spinal cord with TRIzol (Invitrogen) according to the manufacturer's instructions. All gene expression results are expressed as arbitrary units relative to expression of *Actb*. Fold induction of gene expression in spinal cord after EAE induction was determined by dividing the relative abundance of experimental samples by the mean relative abundance of control samples from naive mice. Primer sequence is in supplementary table 1.

ELISA

Thy1.2+ CD4+ T cells FACS-sorted from the brains of wild-type Thy1.1+ recipient mice that received T_H17 cells from MOG-immunized *Asc*$^{f/+}$*Lck*-Cre and *Asc*$^{f/-}$*Lck*-Cre mice, were cultured for 24 hours at 37°C on plates coated with anti-CD3 (3 μg/ml; 553057; BD Pharmingen) and anti-CD28 (3 μg/ml; 553294; BD Pharmingen). Supernatants were collected for enzyme-linked immunosorbent assay of cytokines with a kit from BioLegend (for IL-17A) or kits from R&D Systems (for all other cytokines). *Il1b* levels were assayed by *Il1b* (MLB00C) ELISA kit (R&D systems) according to the manufacturer's instructions. *Ifng* (MIF00), *csf2* (DY415-05) and *Tnf* (MTA00B) ELISA kit were purchased from R&D Systems.

Immunoblot and immunoprecipitation

Cells were lysed by lysis buffer (0.5% Triton X-100, 20 mM Hepes pH 7.4,150 mM NaCl, 12.5 mM β-glycerophosphate, 1.5 mM MgCl2, 10 mM NaF, 2 mM dithiothreitol, 1 mM sodium orthovanadate, 2 mM EGTA, 20 mM aprotinin, 1 mM phenylmethylsulfonyl fluoride). 20 μg of protein lysate per lane was run on a 12% SDS-PAGE gel, followed by immune-blotting with different antibodies. Co-immunoprecipitation experiments were performed as described previously17. In brief, cell extracts were incubated overnight with antibodies and protein A beads at 4 °C After incubation, beads were washed four times with

Author Manuscript Author Manuscript Author Manuscript Author Manuscript

lysis buffer, resolved by SDS-PAGE and analyzed by immunoblotting according to standard procedures.

Statistics

Non-parametric statistics was applied to all data set. The P values of clinical scores were determined by two-way multiple-range ANOVA for multiple comparisons. Other P values were determined by Unpaired t test. $P < 0.05$ was considered to be significant. Unless otherwise specified, all results are shown as mean and the s.e.m. We performed power analysis for a sample size that gives 80% power for an effect size of 1.5. The control and experimental groups were blinded to the investigators who recorded the clinical score, flow analysis, histology and LFB staining. No samples were excluded, and Randomization was not performed.

Supplementary Material

Refer to Web version on PubMed Central for supplementary material.

Acknowledgments

We thank M.D. Wewers and A. Sarkar (Ohio State University College of Medicine) for *Il1b*$^{-/-}$*Il18*$^{-/-}$ mice; Edward S. Mocarski (Emory Vaccine Center) for *Casp8*$^{-/-}$*Rip3*$^{-/-}$ and control mice; Amy G. Hise (Case Western Reserve University) for *Asc*$^{-/-}$, *Nlrp3*$^{-/-}$ and *Il1b*$^{-/-}$ mice. This investigation was supported by a grant from the National Multiple Sclerosis Society (RG5130A2/1) and National Institutes of Health (5R01NS071996-05, 1RO1AA023722 and MSTP-T32GM007250).

References

1. Frohman EM. Multiple sclerosis. The Medical clinics of North America. 2003; 87:867–897. viii–ix. [PubMed: 12834152]
2. Ransohoff RM. Animal models of multiple sclerosis: the good, the bad and the bottom line. Nat Neurosci. 2012; 15:1074–1077. [PubMed: 22837037]
3. Stromnes IM, Cerretti LM, Liggitt D, Harris RA, Goverman JM. Differential regulation of central nervous system autoimmunity by T(H)1 and T(H)17 cells. Nat Med. 2008; 14:337–342. [PubMed: 18278054]
4. Kroenke MA, Carlson TJ, Andjelkovic AV, Segal BM. IL-12- and IL-23-modulated T cells induce distinct types of EAE based on histology, CNS chemokine profile, and response to cytokine inhibition. J Exp Med. 2008; 205:1535–1541. [PubMed: 18573909]
5. Lees JR, Golumbek PT, Sim J, Dorsey D, Russell JH. Regional CNS responses to IFN-gamma determine lesion localization patterns during EAE pathogenesis. J Exp Med. 2008; 205:2633–2642. [PubMed: 18852291]
6. Jager A, Dardalhon V, Sobel RA, Bettelli E, Kuchroo VK. Th1, Th17, and Th9 effector cells induce experimental autoimmune encephalomyelitis with different pathological phenotypes. J Immunol. 2009; 183:7169–7177. [PubMed: 19890056]
7. Cua DJ, et al. Interleukin-23 rather than interleukin-12 is the critical cytokine for autoimmune inflammation of the brain. Nature. 2003; 421:744–748. [PubMed: 12610626]
8. Veldhoen M, Hocking RJ, Atkins CJ, Locksley RM, Stockinger B. TGFbeta in the context of an inflammatory cytokine milieu supports de novo differentiation of IL-17-producing T cells. Immunity. 2006; 24:179–189. [PubMed: 16473830]
9. Mangan PR, et al. Transforming growth factor-beta induces development of the T(H)17 lineage. Nature. 2006; 441:231–234. [PubMed: 16648837]
10. Chung Y, et al. Critical regulation of early Th17 cell differentiation by interleukin-1 signaling. Immunity. 2009; 30:576–587. [PubMed: 19362022]

Author Manuscript Author Manuscript Author Manuscript Author Manuscript

11. Gulen MF, et al. The receptor SIGIRR suppresses Th17 cell proliferation via inhibition of the interleukin-1 receptor pathway and mTOR kinase activation. Immunity. 2010; 32:54–66. [PubMed: 20060329]
12. Staschke KA, et al. IRAK4 kinase activity is required for Th17 differentiation and Th17-mediated disease. J Immunol. 2009; 183:568–577. [PubMed: 19542468]
13. Matsuki T, Nakae S, Sudo K, Horai R, Iwakura Y. Abnormal T cell activation caused by the imbalance of the IL-1/IL-1R antagonist system is responsible for the development of experimental autoimmune encephalomyelitis. Int Immunol. 2006; 18:399–407. [PubMed: 16415102]
14. Gulen MF, et al. Inactivation of the enzyme GSK3alpha by the kinase IKKi promotes AKT-mTOR signaling pathway that mediates interleukin-1-induced Th17 cell maintenance. Immunity. 2012; 37:800–812. [PubMed: 23142783]
15. Chang J, et al. MyD88 is essential to sustain mTOR activation necessary to promote T helper 17 cell proliferation by linking IL-1 and IL-23 signaling. Proc Natl Acad Sci USA. 2013; 110:2270–2275. [PubMed: 23341605]
16. Gris D, et al. NLRP3 plays a critical role in the development of experimental autoimmune encephalomyelitis by mediating Th1 and Th17 responses. J Immunol. 2010; 185:974–981. [PubMed: 20574004]
17. Inoue M, Williams KL, Gunn MD, Shinohara ML. NLRP3 inflammasome induces chemotactic immune cell migration to the CNS in experimental autoimmune encephalomyelitis. Proc Natl Acad Sci USA. 2012; 109:10480–10485. [PubMed: 22699511]
18. Inoue M, et al. Interferon-beta therapy against EAE is effective only when development of the disease depends on the NLRP3 inflammasome. Sci Signal. 2012; 5:ra38. [PubMed: 22623753]
19. Hirota K, et al. Fate mapping of IL-17-producing T cells in inflammatory responses. Nat Immunol. 2011; 12:255–263. [PubMed: 21278737]
20. Arbeloa J, Perez-Samartin A, Gottlieb M, Matute C. P2X7 receptor blockade prevents ATP excitotoxicity in neurons and reduces brain damage after ischemia. Neuro dis. 2012; 45:954–961.
21. Qu Y, et al. Pannexin-1 is required for ATP release during apoptosis but not for inflammasome activation. J Immunol. 2011; 186:6553–6561. [PubMed: 21508259]
22. Gordon GR, et al. Norepinephrine triggers release of glial ATP to increase postsynaptic efficacy. Nat Neurosci. 2005; 8:1078–1086. [PubMed: 15995701]
23. Antonopoulos C, El Sanadi C, Kaiser WJ, Mocarski ES, Dubyak GR. Proapoptotic chemotherapeutic drugs induce noncanonical processing and release of IL-1beta via caspase-8 in dendritic cells. J Immunol. 2013; 191:4789–4803. [PubMed: 24078693]
24. Gringhuis SI, et al. Dectin-1 is an extracellular pathogen sensor for the induction and processing of IL-1beta via a noncanonical caspase-8 inflammasome. Nat Immunol. 2012; 13:246–254. [PubMed: 22267217]
25. Bossaller L, et al. FAS (CD95) mediates noncanonical IL-1beta and IL-18 maturation via caspase-8 in an RIP3-independent manner. J Immunol. 2012; 189:5508–5512. [PubMed: 23144495]
26. Oberst A, et al. Catalytic activity of the caspase-8-FLIP(L) complex inhibits RIPK3-dependent necrosis. Nature. 2011; 471:363–367. [PubMed: 21368763]
27. Leverrier S, Salvesen GS, Walsh CM. Enzymatically active single chain caspase-8 maintains T-cell survival during clonal expansion. Cell Death Differ. 2011; 18:90–98. [PubMed: 20523353]
28. Bell BD, et al. FADD and caspase-8 control the outcome of autophagic signaling in proliferating T cells. Proc Natl Acad Sci USA. 2008; 105:16677–16682. [PubMed: 18946037]
29. Kang TB, et al. Caspase-8 serves both apoptotic and nonapoptotic roles. J Immunol. 2004; 173:2976–2984. [PubMed: 15322156]
30. Salmena L, et al. Essential role for caspase 8 in T-cell homeostasis and T-cell-mediated immunity. Genes Dev. 2003; 17:883–895. [PubMed: 12654726]
31. Chun HJ, et al. Pleiotropic defects in lymphocyte activation caused by caspase-8 mutations lead to human immunodeficiency. Nature. 2002; 419:395–399. [PubMed: 12353035]
32. Bauernfeind FG, et al. NF-kappaB activating pattern recognition and cytokine receptors license NLRP3 inflammasome activation by regulating NLRP3 expression. J Immunol. 2009; 183:787–791. [PubMed: 19570822]

Author Manuscript Author Manuscript Author Manuscript Author Manuscript

33. Martin BN, et al. IKKalpha negatively regulates ASC-dependent inflammasome activation. Nat Commun. 2014; 5:4977. [PubMed: 25266676]
34. Bryan NB, Dorfleutner A, Rojanasakul Y, Stehlik C. Activation of inflammasomes requires intracellular redistribution of the apoptotic speck-like protein containing a caspase recruitment domain. J Immunol. 2009; 182:3173–3182. [PubMed: 19234215]
35. Schenten D, et al. Signaling through the adaptor molecule MyD88 in CD4+ T cells is required to overcome suppression by regulatory T cells. Immunity. 2014; 40:78–90. [PubMed: 24439266]
36. Doitsh G, et al. Cell death by pyroptosis drives CD4 T-cell depletion in HIV-1 infection. Nature. 2014; 505:509–514. [PubMed: 24356306]
37. Shaw PJ, et al. Critical role for PYCARD/ASC in the development of experimental autoimmune encephalomyelitis. J Immunol. 2010; 184:4610–4614. [PubMed: 20368281]
38. El-Behi M, et al. The encephalitogenicity of T(H)17 cells is dependent on IL-1- and IL-23-induced production of the cytokine GM-CSF. Nat Immunol. 2011; 12:568–575. [PubMed: 21516111]
39. Qian Y, et al. The adaptor Act1 is required for interleukin 17-dependent signaling associated with autoimmune and inflammatory disease. Nat Immunol. 2007; 8:247–256. [PubMed: 17277779]
40. Kang Z, et al. Astrocyte-restricted ablation of interleukin-17-induced Act1-mediated signaling ameliorates autoimmune encephalomyelitis. Immunity. 2010; 32:414–425. [PubMed: 20303295]
41. Wei DG, et al. Expansion and long-rangedifferentiation of the NKT cell lineage in mice expressing CD1d exclusively on cortical thymocytes. J Exp Med. 2005; 202:239–48. [PubMed: 16027237]
42. Shornick LP, et al. Mice deficient in IL-1beta manifest impaired contact hypersensitivity to trinitrochlorobenzone. J Exp Med. 1996; 183:1427–36. [PubMed: 8666901]
43. Tomalka J, et al. A Novel Role for the NLRC4 Inflammasome in Mucosal Defenses against the Fungal Pathogen Candida albicans. PLoS Pathog. 2011; 7:e1002379. [PubMed: 22174673]
44. Anasuya S, et al. Caspase-1 regulates Escherichia coli sepsis and splenic B cell apoptosis independent of interleukin-1β and interleukin-18. Am J Respir Crit Care Med. 2006; 174:1003–1010. [PubMed: 16908867]
45. Kuida K, et al. Altered cytokine export and apoptosis in mice deficient in interleukin-1 beta converting enzyme. Science. 1995; 267:2000–3. [PubMed: 7535475]
46. William, J Kaiser, et al. RIP3 mediates the embryonic lethality of caspase-8-deficient mice. Nature. 2011; 471:368–372. [PubMed: 21368762]
47. Shiho, Suzuki, et al. Shigella Type III Secretion Protein MxiI Is Recognized by Naip2 to Induce Nlrc4 Inflammasome Activation Independently of Pkcd. PLoS Pathog. 2014; 10:e1003926. [PubMed: 24516390]

Author Manuscript Author Manuscript Author Manuscript Author Manuscript

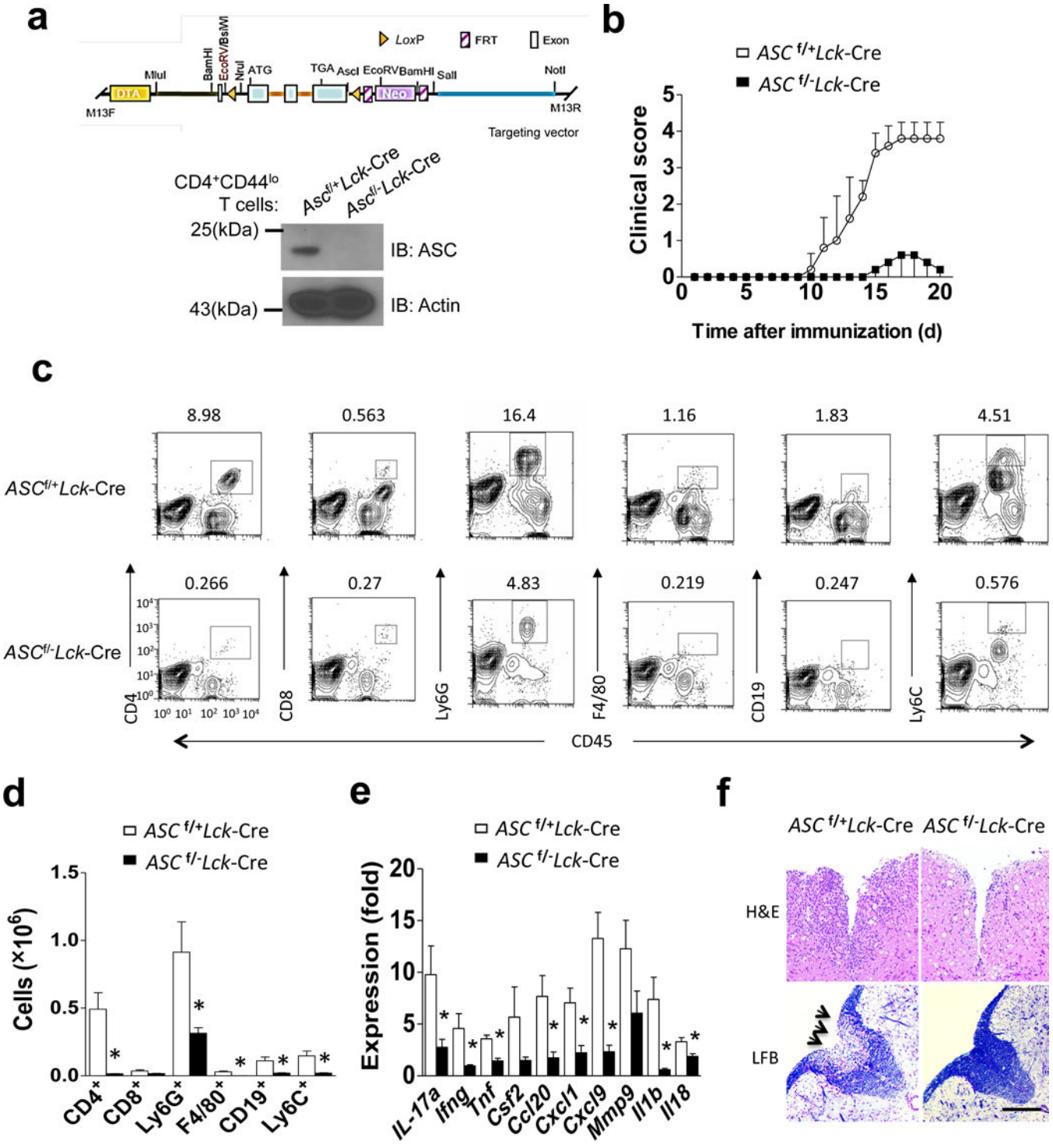

Figure 1.

Genetic deletion of the inflammasome adaptor ASC in T cells protects from EAE. (**a**) Targeting vector design for generation of a novel mouse strain with all three *Pycard* exons flanked by lox(p) sites (upper panel), and Western blot analysis of ASC expression in FACS-sorted naïve CD4+ T cells from *Asc*$^{f/+}$*Lck*-Cre and *Asc*$^{f/-}$*Lck*-Cre mice (lower panel). (**b**)

Author Manuscript Author Manuscript Author Manuscript Author Manuscript

Mean clinical score of EAE in *Asc*$^{f/+}$*Lck*-Cre and *Asc*$^{f/-}$*Lck*-Cre mice (n=5 mice per group) induced by active immunization with $MOG_{35–55}$. (**c–d**) Immune cell infiltration in the brains of $MOG_{35–55}$-immunized *Asc*$^{f/+}$*Lck*-Cre and *Asc*$^{f/-}$*Lck*-Cre mice (n = 5, 7 days after disease onset) was analyzed by flow cytometry with the antibodies as indicated. (**d**) Absolute numbers of CNS-infiltrating cells were determined at the peak of disease. Brains and spinal cords were harvested together and mononuclear infiltrating cells were stained with the indicated antibodies, followed by flow cytometric analysis. (**e**) Real-time PCR analysis of inflammatory gene expression as indicated in the spinal cords of *Asc*$^{f/+}$*Lck*-Cre and *Asc*$^{f/+}$*Lck*-Cre mice (n=5) at the peak of disease. (**f**) Hematoxylin and eosin (H&E) staining (upper panels) and Luxol fast blue staining (lower panels) of lumbar spinal cords from *Asc*$^{f/+}$*Lck*-Cre and *Asc*$^{f/-}$*Lck*-Cre mice harvested at the peak of disease. Scale bar, 200μm. *P < 0.05 (Unpaired t test**, d and e**). *P < 0.05 (Two-way ANOVA,**b**). Data are representative of three independent experiments. Error bars represent s.d (**b**). Error bars represent s.e.m (**d**,**e**). 5 mice per group in each experiment.

Author Manuscript Author Manuscript Author Manuscript Author Manuscript

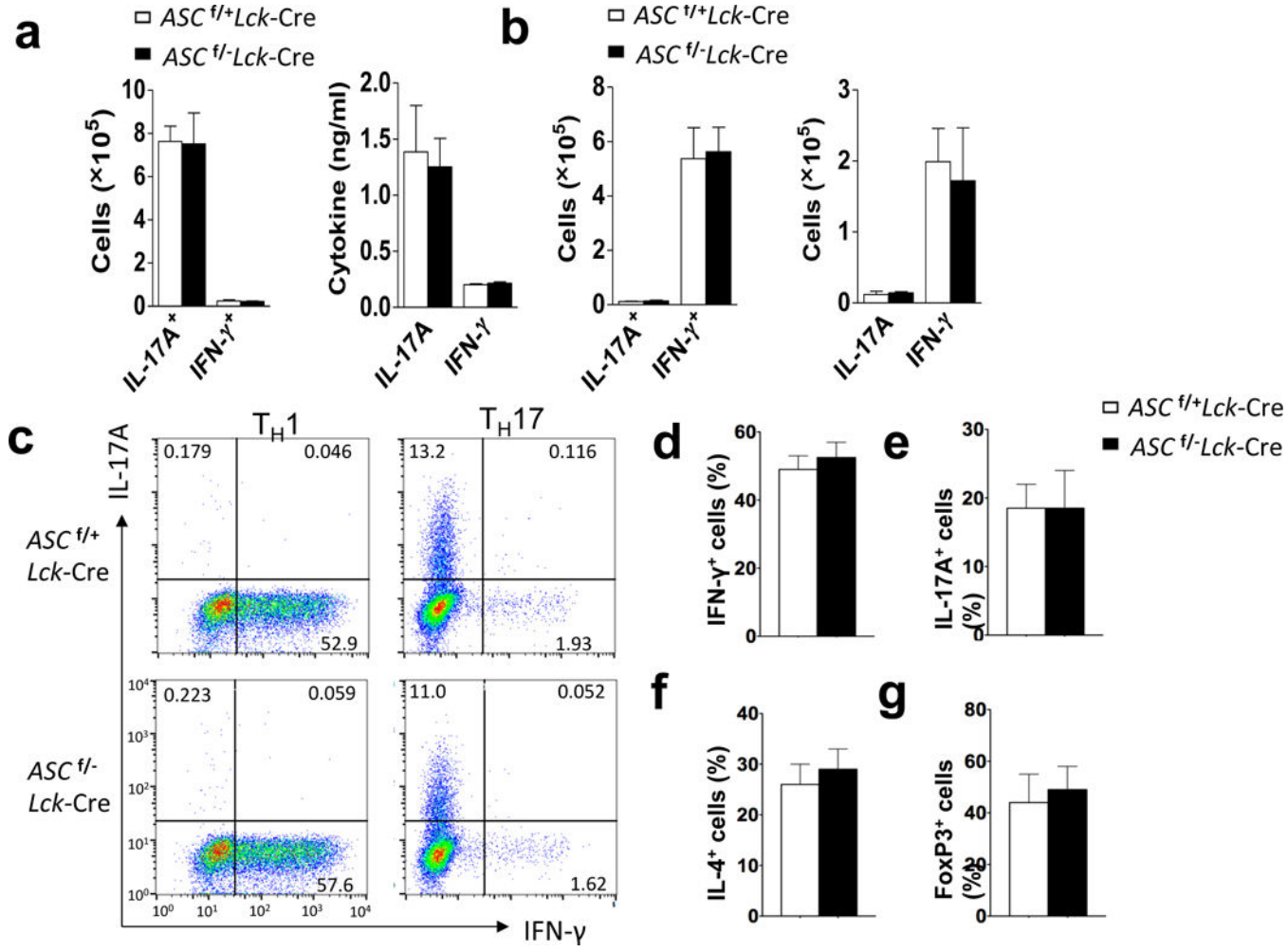

Figure 2.

MOG-reactive T effector cell priming in the secondary lymphoid organs is unaffected by ASC deficiency in T cells. (**a**) Absolute numbers of CD4+ IL-17A+ and CD4+ IFN-γ+ cells (left panel) and concentrations of IL-17A and IFN-γ in the supernatant of cells (right panel) from the draining lymph nodes of mice (n=5 mice per group) 10 days after immunization with $MOG_{35–55}$, followed by *ex vivo* re-stimulation in the presence of $MOG_{35–55}$ and IL-23. (**b**) Absolute numbers of CD4+IL-17A+ and CD4+IFN-γ+ cells **(left panel)** and concentrations of IL-17A and IFN-γ in the supernatant of cells **(right panel)** from the draining lymph nodes of mice (n=5) 10 days after immunization with $MOG_{35–55}$,, followed by *ex vivo* restimulation in the presence of $MOG_{35–55}$ and IL-12. (**c**) FACS-sorted naïve ($CD4^+CD44^{lo}$) CD4+ T cells were cultured on an anti-CD3/CD28 coated plate in T_H17- or T_H1-polarizing condition, followed by intracellularly staining for IL-17A and IFN-γ and analyzed by flow cytometry. (**d–g**) Mean percentage of cells positive for the indicated cytokines/protein following intracellular staining with the indicated antibodies and flow cytometric analysis on day 3 of in vitro differentiation of T_H1 (**d**), T_H17 (**e**), T_H2 (**f**), and Treg (**g**) cell populations**.** Data are representative of three independent experiments (**a–g**). n=5 mice per group in each experiment (**a–b**) and n=3 mice per group in each experiment (**c–g**).

Author Manuscript Author Manuscript Author Manuscript Author Manuscript

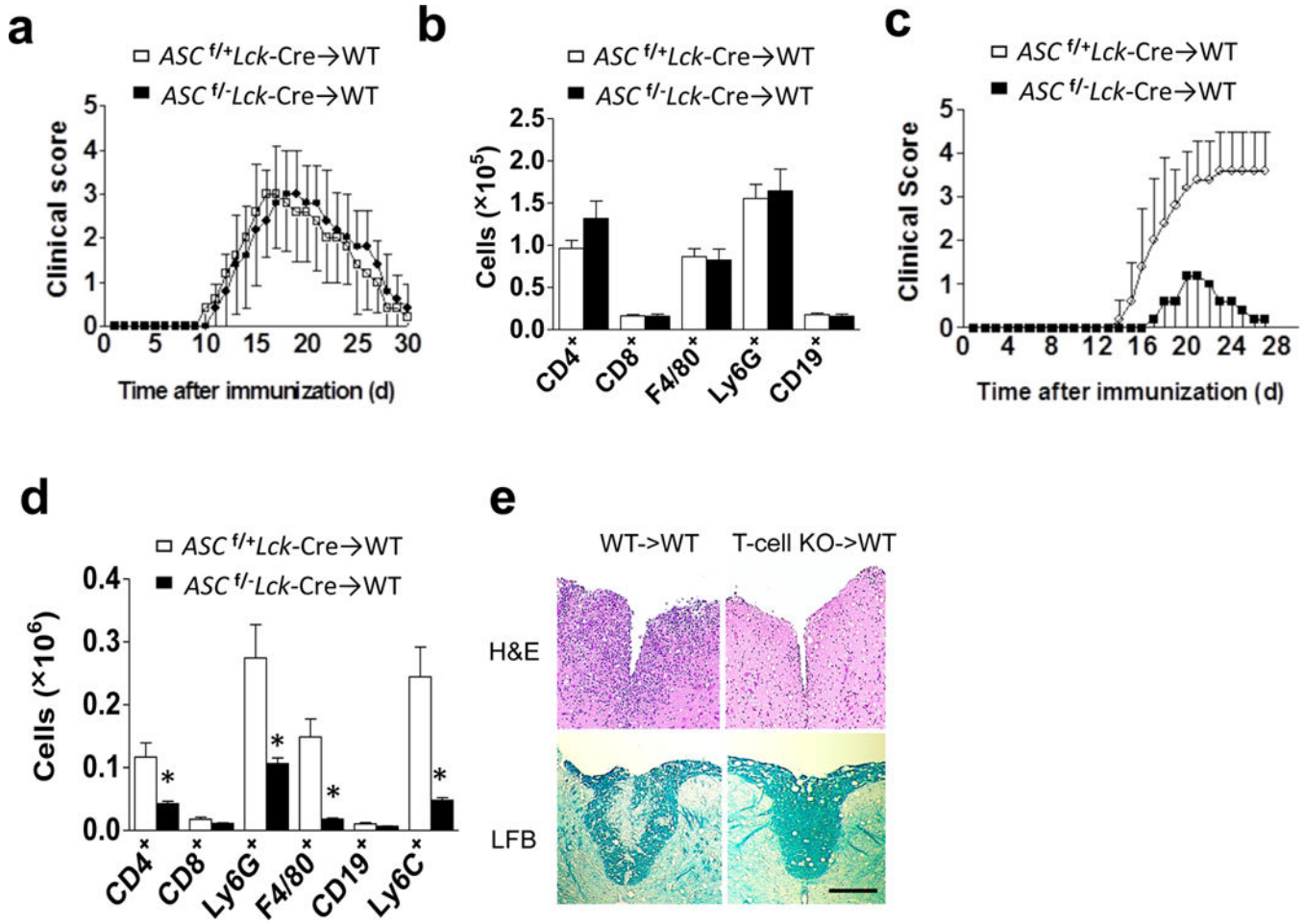

Author Manuscript Author Manuscript Author Manuscript Author Manuscript

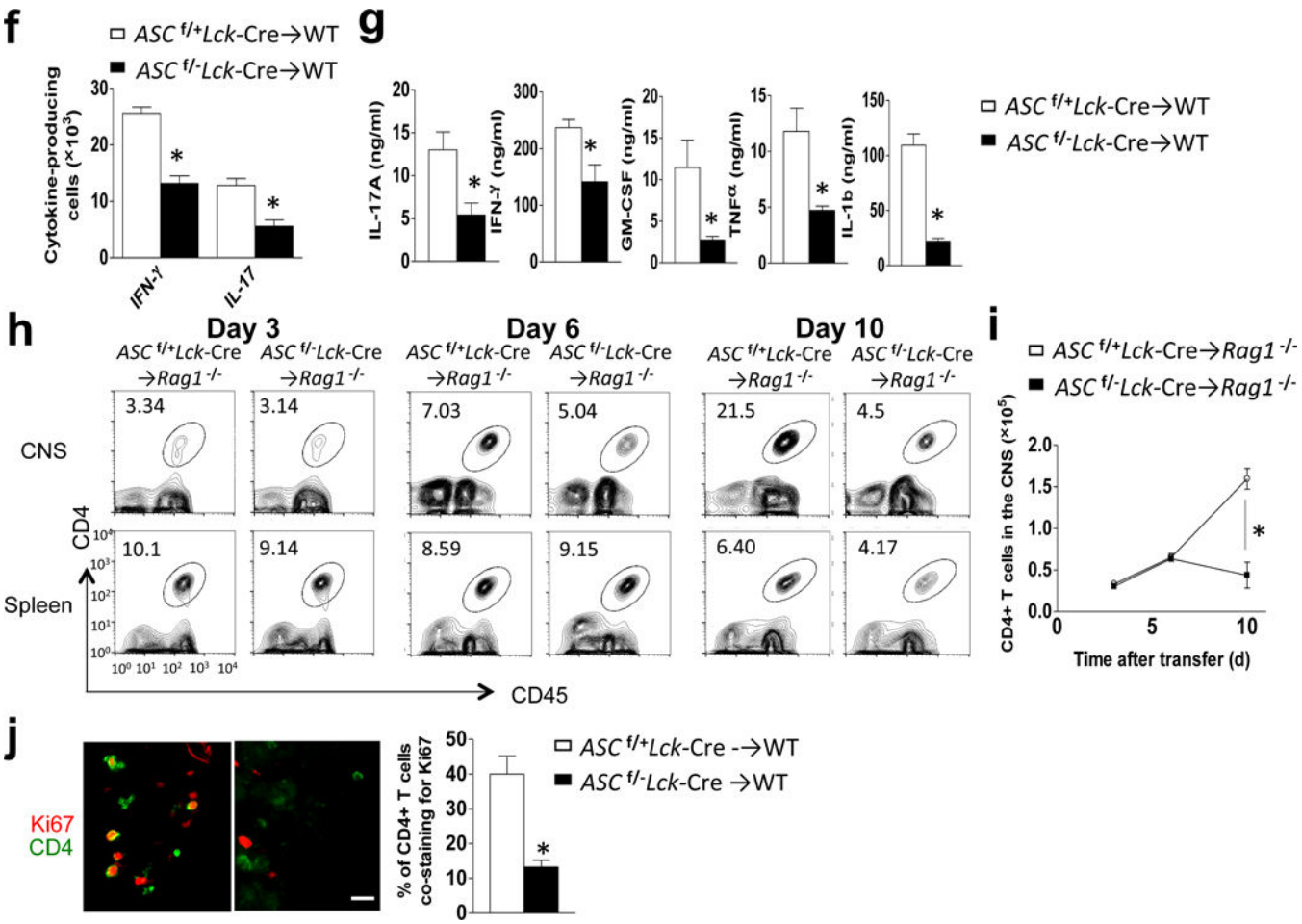

Figure 3.

T cell specific ASC deficiency is required for T_H17- but not T_H1-mediated EAE. (**a,c**) Mean clinical score of EAE mice (n=5) induced by adoptive transfer of MOG-reactive T_H1 (**a**) and T_H17 (**c**) cells. (**b, d**) Brains and spinal cords T_H1- (**b**) and T_H17- (**d**) recipient mice were harvested at the peak of disease and stained with the antibodies, followed by flow cytometric analysis. (**e**) H&E staining (upper panels) and Luxol fast blue staining (lower panels) of lumbar spinal cords at peak of the disease in T_H17 recipient mice. Scale bar, 200μm**.** (**f**) Flow cytometric analysis of CD4+ cells from the brains of wild-type mice at peak of the disease in T_H17 recipient mice. (**g**) Thy1.2+ CD4+ T cells FACS-sorted from the brains of Thy1.1+ T_H17 recipient mice (n=5), were cultured and analyzed by ELISA. (**h**) Flow cytometric analyses of CD4+ T cells from CNS or spleen from *Rag*$^{-/-}$ mice (n=5) that received MOG-reactive T_H17 cells. (**i**) Quantification of total CNS-infiltrating CD4+ T cells from (**h**). (**j**) Ki-67/CD4 staining of spinal cords from adoptive transfer experiments from (**h**) (**left panels**), and percentage of CD4+ T cells co-staining with Ki-67 (**right panel**). Scale bar, 10μm. Error bars represent s.e.m. *P < 0.05 (Unpaired t test for **b, d, f, g, l** and **j**). Error bars represent s.d. *P < 0.05 (Two-way ANOVA for **a** and **c**). Data are representative of three independent experiments (**a–j**). n=5 mice per group in each experiment.

Author Manuscript Author Manuscript Author Manuscript Author Manuscript

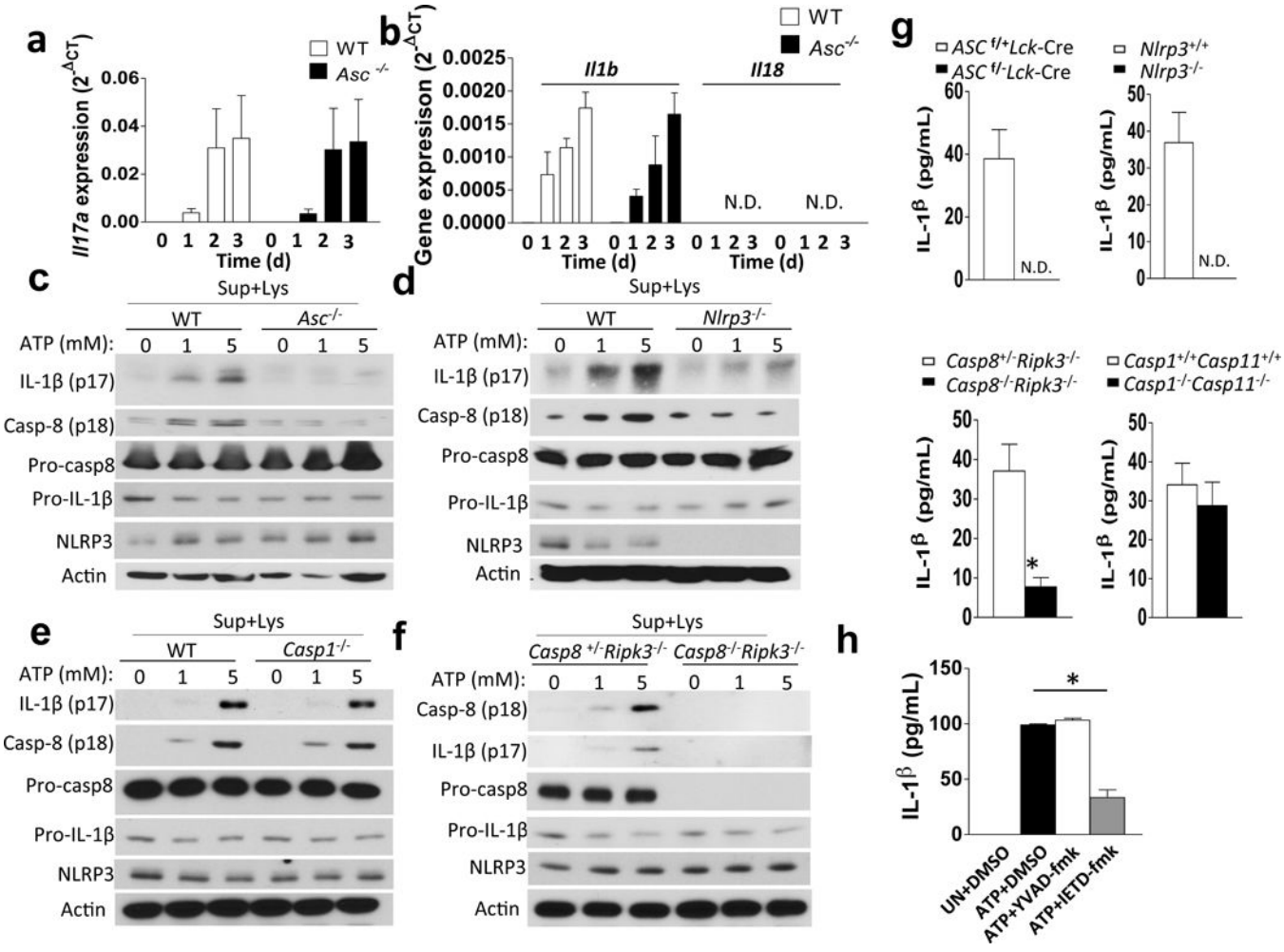

Author Manuscript Author Manuscript Author Manuscript Author Manuscript

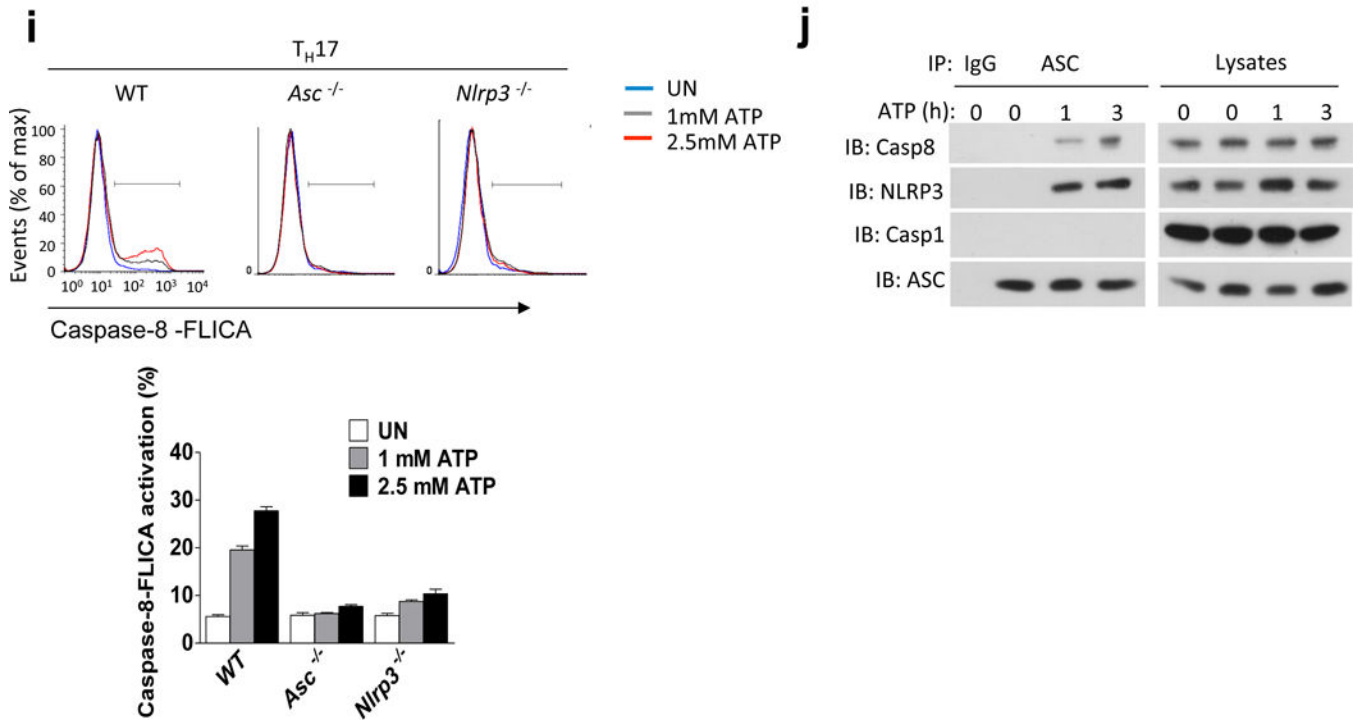

Figure 4.

T_H17 cells process IL-1β in response to stimulation with extracellular ATP in an ASC/NLRP3/Caspase-8-dependent manner. (**a–j**) FACS-sorted ($CD4^+CD44^{lo}$) naïve CD4+ T cells were subjected to T_H17 polarization. (**a, b**) T_H17 cells were analyzed by real-time PCR analysis of the indicated genes. (**c–f**) T_H17 cells were stimulated with ATP (8 h), and cells were lysed, followed by Western analysis with the indicated antibodies. (**g**) T_H17 cells were stimulated with ATP (8 h), and IL-1β ELISA was performed on cell-free supernatants. (**h**) T_H17 cells were treated with the indicated inhibitors and ATP (8 h), followed by IL-1β ELISA. (**i**) T_H17 cells were stimulated with ATP for 8 h; caspase-8 FLICA (IETD) reagent was added directly to the media for the last hour of incubation. Cells were then harvested and analyzed by flow cytometry (upper). Qutification of Caspase 8 FLICA activation (lower). (**j**) T_H17 cells were stimulated with 1 mM ATP for 0, 1, or 3 h. Cells were then harvested and lysed, followed by immunoprecipitation with anti-ASC antibody and Western blot with indicated antibodies. n=5 mice per group in each experiment. n=2 mice per group in each experiment (**i**). Error bars represent s.e.m. *P < 0.05 (Unpaired t test for **a, b, g, h** and **j**). Data are representative of three independent experiments (**a–j**).

Author Manuscript
Author Manuscript
Author Manuscript
Author Manuscript

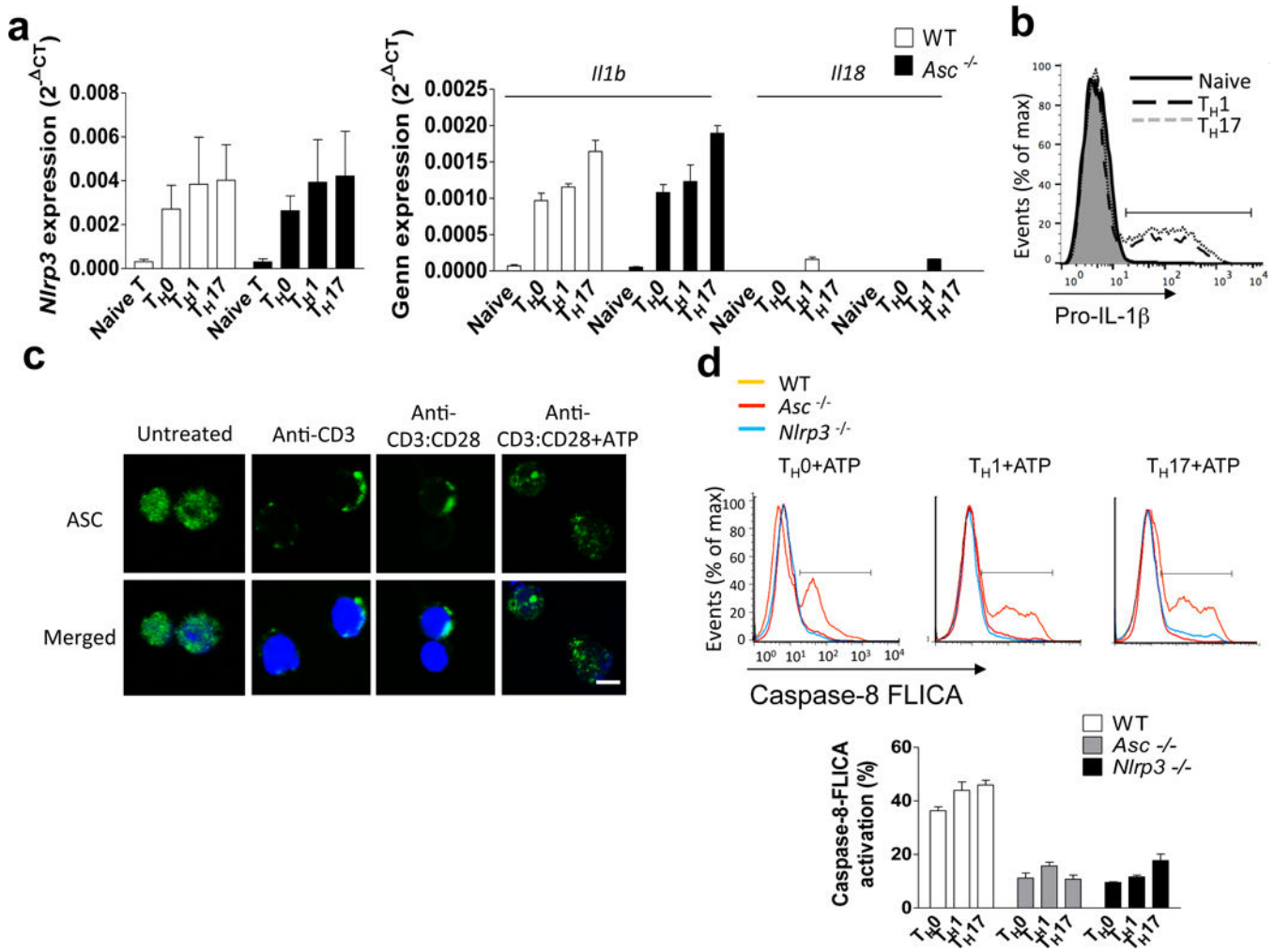

Author Manuscript Author Manuscript Author Manuscript Author Manuscript

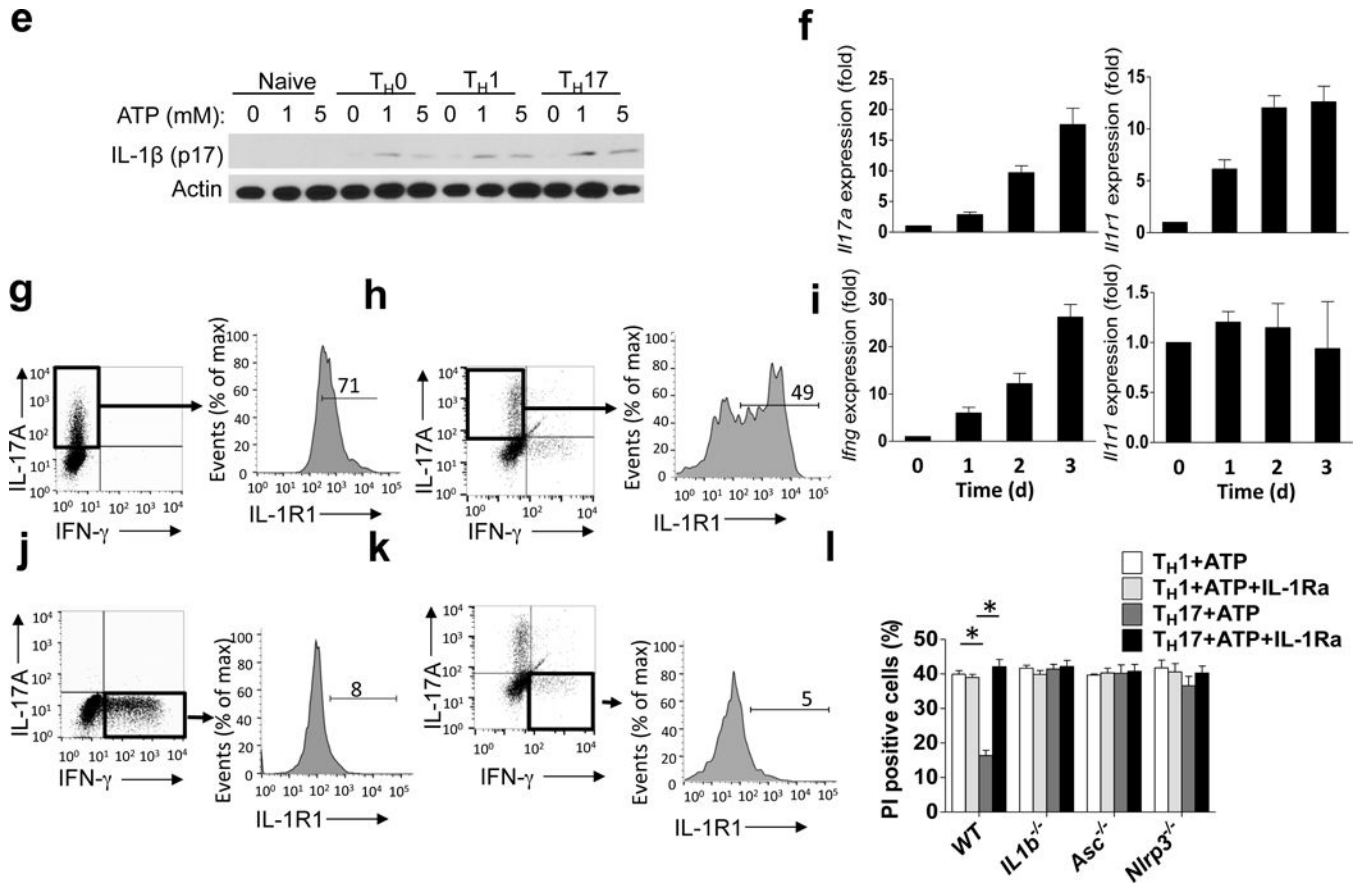

Figure 5.

T_H17 cells express IL-1R and pro-IL-1β. (**a**) mRNA expression for the indicated genes in naïve CD4+ T cells, T_H0, T_H1 and T_H17 cells. (**b**) Naïve CD4+ T cells, T_H1 and T_H17 cells were stained for pro-IL-1β and analyzed by flow cytometry. (**c**) Naive CD4+ T cells were stimulated with the antibodies, followed by staining with anti-ASC and confocal microscopic analysis. Scale bar, 5μm**.** (**d**) T_H0, T_H1 and T_H17 cells were treated with 5 mM ATP for 8 h; caspase-8 FLICA (IETD) was added, followed by flow cytometry. (**e**) Naive CD4+ T cells, T_H0, T_H1 and T_H17 cells were treated with ATP for 8 h. Cell lysates were immunoblotted with the antibodies. (**f, i**) T_H1 and T_H17 cells were analyzed by real-time PCR on days 0–3 of differentiation. (**g, j**) T_H17 (**g**) and T_H1 (**j**) cells were stained with the indicated antibodies and analyzed by flow cytometry. (**h, k**) Cells of draining lymph nodes from MOG-immunized mice were analyzed by flow cytometric analysis with the indicated antibodies. (**l**) T_H1 and T_H17 cells were pre-treated for 15 minutes with IL-1ra (1 μg/ml), then stimulated with 5 mM ATP for 8 h. Cells were stained with propidium iodide and analyzed by flow cytometry. Error bars represent s.e.m. *P < 0.05 (Unpaired t test for **a, d, f, i, l**). Data are representative of three independent experiments (**a–i**). n=5 mice per group in each experiment (**b, g–h, j–l**). n=2 mice per group in each experiment (**a, d, f and i**).

Author Manuscript Author Manuscript Author Manuscript Author Manuscript

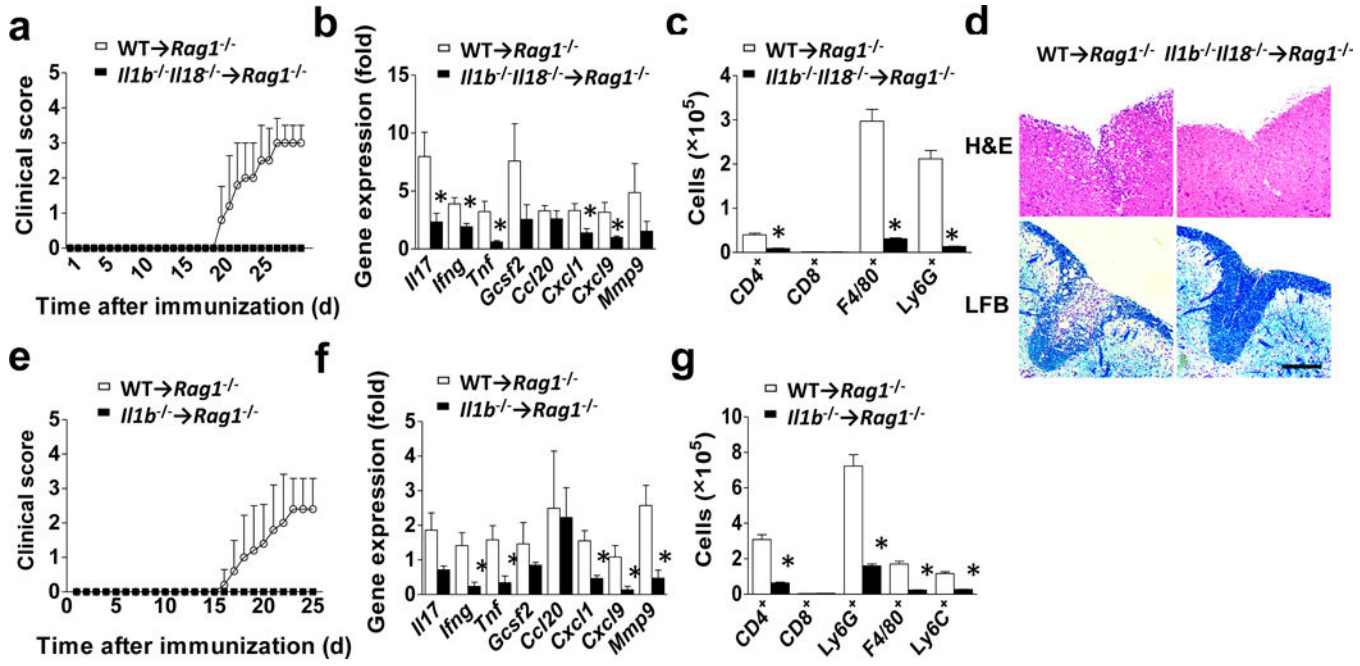

Figure 6.

IL-1β produced by CD4+ T cells in vivo. (**a–e**) *Rag1*$^{-/-}$ mice (n=5 mice per group) were reconstituted with 2×10^6 sorted CD4+ T cells from wild-type or *Il1b*$^{-/-}$*Il18*$^{-/-}$ mice, followed by immunization with MOG$_{35–55}$ peptide. (**a**) Mean clinical score. (**b**) Inflammatory gene expression in the lumbar spinal cord was assessed at the peak of disease. (**c**) Absolute numbers of CNS-infiltrating cells were determined at the peak of disease. Brains and spinal cords were harvested and mononuclear infiltrating cells were stained with the indicated antibodies, followed by flow cytometric analysis. (**d**) H&E staining (**upper panels**) and Luxol fast blue staining (**lower panels**) of lumbar spinal cords from *Rag1*$^{-/-}$ recipient mice harvested at the peak of disease. Scale bar, 200μm**.** (**e–g**) *Rag1*$^{-/-}$ mice were reconstituted with 2×10^6 sorted CD4+ T cells from wild-type or *Il1b*$^{-/-}$ mice, followed by immunization with MOG$_{35–55}$ peptide. (**e**) Mean clinical score. (**f**) Inflammatory gene expression in the lumbar spinal cord was assessed at the peak of disease. (**g**) Absolute numbers of CNS-infiltrating cells were determined at the peak of disease. Brains and spinal cords were harvested and mononuclear infiltrating cells were stained with the indicated antibodies, followed by flow cytometric analysis. Error bars represent s.e.m. *P < 0.05 (Unpaired t test for **b, c, f** and **g**). Error bars represent s.d. *P < 0.05 (Two-way ANOVA for **a** and **e**). Data are representative of three independent experiments (**a–g**). n=5 mice per group in each experiment.

Author Manuscript Author Manuscript Author Manuscript Author Manuscript

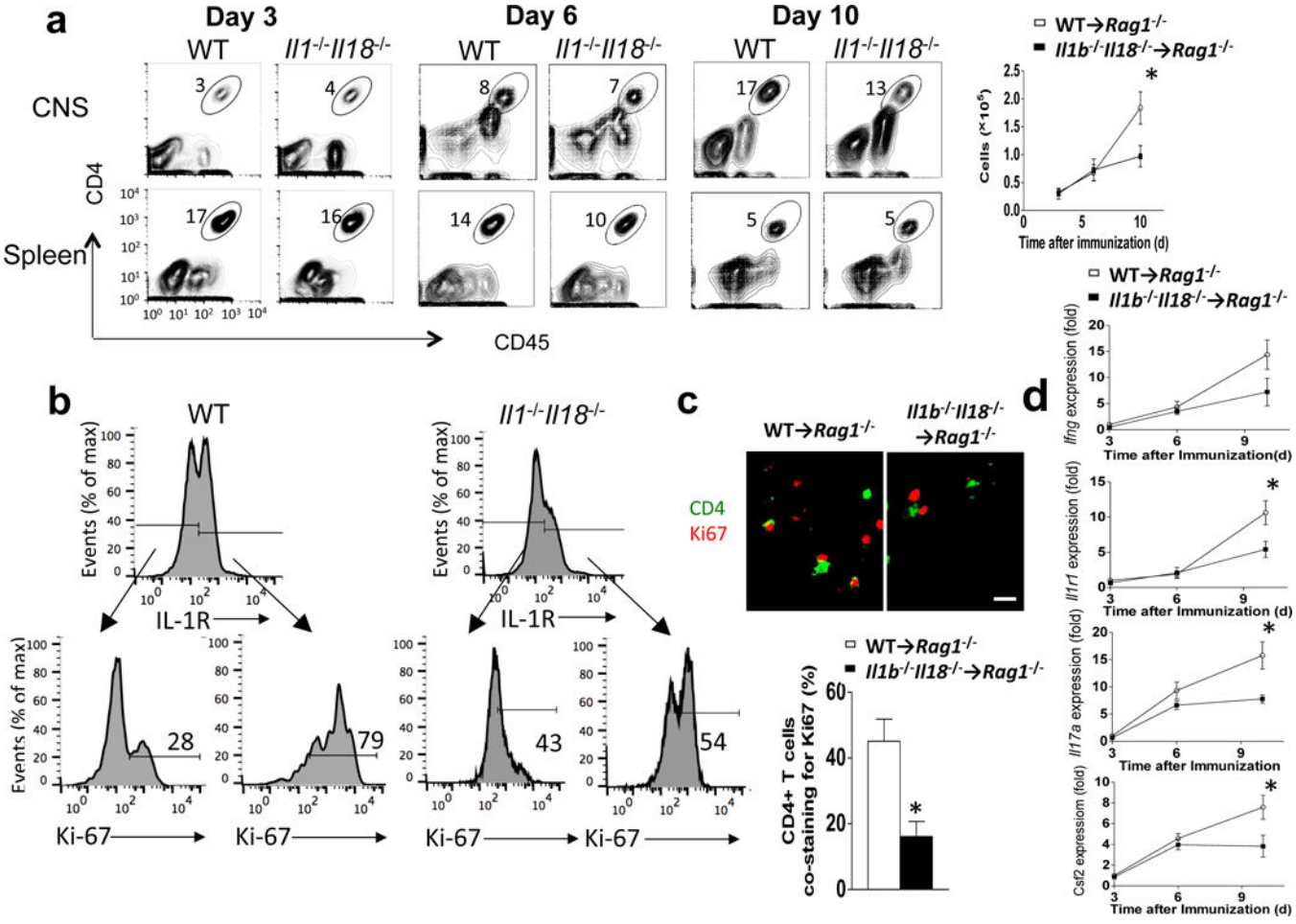

Figure 7.

T cell-intrinsic inflammasome activation is required for T_H17 cell survival/proliferation in the CNS. (**a–d**) *Rag1*$^{-/-}$ mice were reconstituted with 2×10^6 wild-type or *Il1b*$^{-/-}$*Il18*$^{-/-}$ CD4+ T cells. *Rag1*$^{-/-}$ mice were actively immunized with $MOG_{35–55}$ peptide. (**a**) Flow cytometric analysis of CD4+ T cells from CNS or spleen harvested on the indicated day (post-transfer) from *Rag1*$^{-/-}$ mice (n=5 mice per group) that received MOG-reactive T_H17 cells from wild-type and *Il1b*$^{-/-}$*Il18*$^{-/-}$ mice (**left panels**). Quantification of total CNS-infiltrating CD4+ cells on indicated day (**right panel**). (**b**) CNS-infiltrating CD4+ T cells were isolated on day 10 after the last immunization, and were stained with anti-IL-1R and anti-Ki-67 antibodies, followed by flow cytometry. (**c**) Anti-CD4 and anti-Ki-67 immunostaining was performed on spinal cords on day 10 after immunization (**upper panels**). The percentage of CD4+ cells co-staining with Ki67 was calculated for each experimental group (**lower panel**). Scale bar, 10μm. (**d**) Gene expression analysis of lumbar spinal cords obtained from *Rag1*$^{-/-}$ recipient mice on the indicated day post-immunization. Error bars represent s.e.m. *P < 0.05 (Unpaired t test for **a, c** and **d).** Data are representative of three independent experiments (**a–d**). n = 5 mice per group in each experiment.